

Original Research

Responses of Ambient Ozone and Other Pollutants to COVID-19 Lockdown in Taiyuan, North China

Jie Ren*, Xinya Zhao, Xiaoxin Guo, Fengbo Guo, Kankan Liu**

School of Environment and Safety Engineering, North University of China, Taiyuan, 030051, China

Received: 10 September 2021

Accepted: 13 November 2021

Abstract

Coronavirus Disease 2019 (COVID-19) lockdown was related to a significant reduction in air pollutant emissions. However, severe air pollution events still occurred frequently in Taiyuan, north China. To better understand this unusual phenomenon, O₃ and other pollutants have been investigated before, during and after the COVID-19 lockdown in the early 2020. Results show that PM₁₀, PM_{2.5}, SO₂, NO₂ and CO underwent a more marked reduction while O₃ pollution was amplified during lockdown and the average concentrations O₃-8hr during AL stage (101.92 µg m⁻³) exceeded its Grade I limiting value (100 µg m⁻³). O₃ were negatively correlated with the other pollutants and positively correlated with temperature, visibility and the average solar irradiance during the daytime. The increase in daylight hours and average solar irradiance might be the key factors leading to the increase in O₃ concentrations. The reduction of PM_{2.5} and NO₂ promoted the rise in O₃ during the lockdown. The majority of the O₃ was likely formed by photooxidation in the shadow of Taiyuan and linked with air masses from the northern part of Shanxi Province before the lockdown and Henan, Hebei and Shandong during and after the lockdown.

Keywords: ozone, COVID-19, lockdown, backward trajectories, PSCF

Introduction

China's pollution of air has been a worldwide attention for decades [1]. As the largest developing country in the world, China has experienced rapid economic growth over the past few decades, however, energy consumption such as coal combustion, industrial waste and motor vehicles usage have increased, and urban planning and construction have

been accompanied by rapid economic development have all caused environmental air pollution in China, making it one of the most polluted countries in the world [2]. To mitigate the severe air contamination problems, the Chinese governance has promulgated a variety of air quality management (LAQM) and control policies for major pollution sources [3], such as installation of flue gas desulfurization and denitrification control devices in coal-fired power plants, coal-to-gas conversion, and stricter emission standards for automobiles and industrial boilers [4]. China has indeed effectively controlled and reduced most air pollutants' concentrations these years [5].

*e-mail: s1914020@st.nuc.edu.cn

**e-mail: liukk@nuc.edu.cn

From the analysis of annual concentrations of standard air contaminants ($PM_{2.5}$, PM_{10} , sulphur dioxide (SO_2), nitrogen dioxide (NO_2), carbon monoxide (CO), and ground-level ozone (O_3)) in the 74 key cities (the total population in these cities accounted for around 41.2% of China's population in 2017) in China from 2013 to 2017 [2], there were large reductions in annual average concentrations of $PM_{2.5}$, PM_{10} , SO_2 and CO and slight decline in NO_2 concentrations. However, O_3 pollution and associated impacts on health have become serious contemporaneously because of its significant increases in average annual concentrations [2, 5]. Since human activities are one of the main sources that emit these major standard pollutants into the atmosphere [6], it is expected that the lockdown reduce the concentration of these pollutants in the atmosphere with the expansion of the coronavirus disease 2019 (COVID-19, initially identified in Wuhan in early December 2019) [7-9]. Due to the pandemic of COVID-19, whole China was under a special lockdown, because most people were confined to their homes to stop the spread of COVID-19, leading to large reductions in population movement and industrial processes (i.e. the Spring Festival holiday was prolonged to after February 10th, the schools, all entertainment venues, restaurants, and most enterprises were shut down). Mobility, industrial output and energy demand kept up many less than normal levels. The reduction in the combustion of industrial coal and petroleum was related to a significant reduction in the emissions of air pollutants from combustion [6], however, widespread ambient air pollution still occurred over China [10, 11], indicating the generation of them should be influenced not only by emission reduction and also multiple factors else.

China's surface O_3 pollution has attracted widespread attention because O_3 is the unique air quality index (AQI) that has maintained an upward trend in recent years [2, 12]. Because of its strong oxidation, ground-level O_3 has negative influence on air quality and ecosystem [13]. Meanwhile, like carbon dioxide (CO_2), O_3 is also an important greenhouse gas [14]. Ambient O_3 is a characteristic secondary pollutant,

mainly from photochemical reaction against volatile organic compounds (VOCs) and nitrogen oxides (NO_x , $NO + NO_2$) under high temperatures and sunlight [15] and photochemistry of O_3 production has a highly non-linear relationship between volatile organic pollutants (VOCs) and NO_x . The unprecedented emission reduction with relatively low temperatures and sunlight in early 2020 is a rare real-life experiment for exploring the causes of the increase of O_3 surface levels. As the capital city of the Shanxi province with heavy depend on coal as a major source of heat and electricity in the North China, Taiyuan implemented a range of measures to control the transmission of infections during the COVID-19 eruption in early 2020, providing a chance to comprehend the impact on the COVID-19 lockdown on the increase of surface levels of O_3 and other general air pollutants in the North China.

Therefore, we analysed the characteristics of O_3 and other five general air pollutants (including PM_{10} , $PM_{2.5}$, SO_2 , NO_2 and CO) and meteorological factors. We also discussed the correlations among air pollutants as well as meteorological parameters and the influence of air mass transportation on pollutants. This study will provide reference for a comprehensive assessment of the impact of lockdown responses. The study results are not only relevant for the responses of ambient O_3 and other pollutants to COVID-19 lockdown, they also are a starting point for discussing mitigation strategies.

Material and Methods

Study Area Description

Taiyuan (111°30'~113°09'E, 37°27'~38°25'N), a typical city of heavy reliance on coal as its main source of heat and power, is located in the north of Fenhe plain with a population of approximately 4.2 million. Its urban and rural land areas are respectively ~1500 km² and ~5500 km², and the terrain resembles a bowl surrounded by hills in its west, north, and east directions. The sampling site is located in the

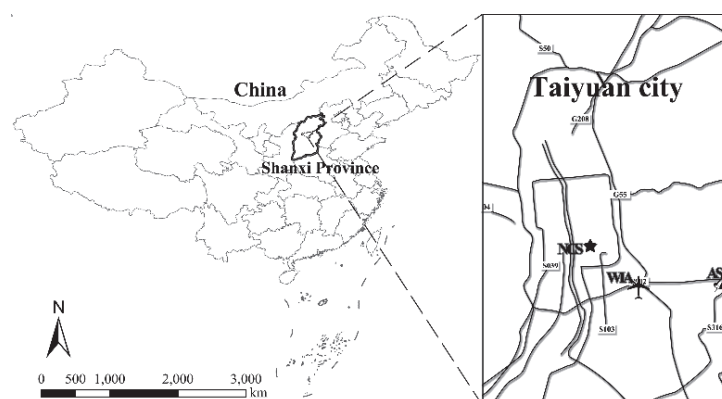


Fig. 1. The national controlling air sampling site (NCS, star) with Wusu international airport (WIA, plane) and agrometeorological station (AS, pin).

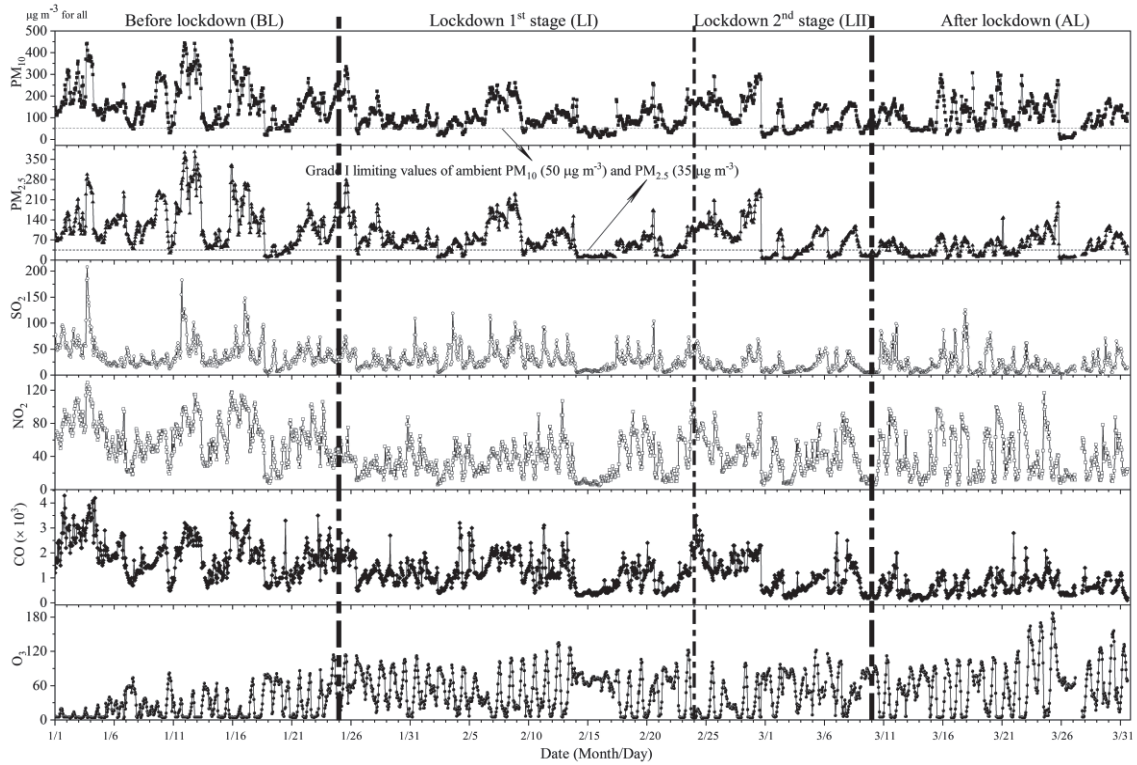


Fig. 2. Hourly concentrations of PM_{10} , $PM_{2.5}$, SO_2 , NO_2 , CO and O_3 .

to the receptor site along the trajectory via back trajectory of the air parcel passing through this location. The zone of concern is divided into $i \times j$ small equal grid cells. The PSCF value in the cell (i, j) is defined as

m_{ij}/n_{ij} , where n_{ij} is denoted as the number of times that the trajectories passed through the cell (i, j) and m_{ij} is the numbers of “polluted” trajectory endpoints in the same cell [18]. Cells with high PSCF values are related to

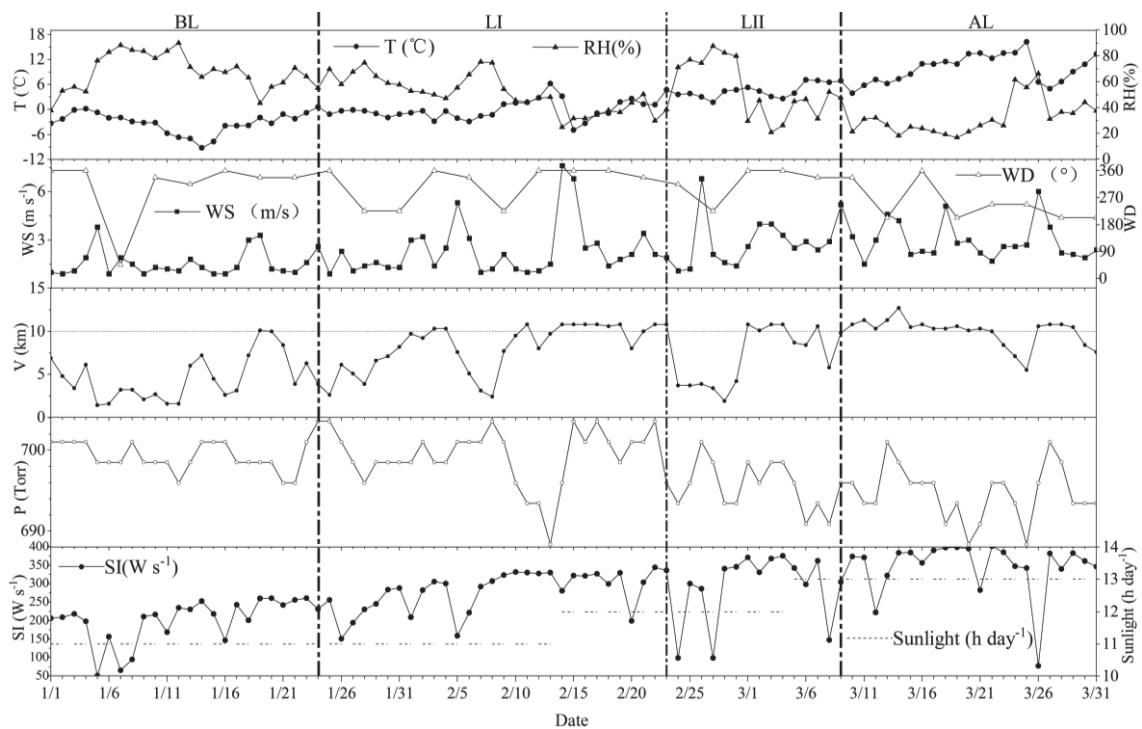


Fig. 3. Daily values of temperature (T), relative humidity (RH), wind speed (WS) and direction (WD), visibility (V), pressure (P), average solar irradiance (SI) and daily hours of sunlight during BL, LI, LII and AL stages.

the arrival of air parcels at a receptor site with pollutant concentrations higher than a given value. These cells indicate areas that have a ‘high potential’ contributions to the pollution at a receptor site [21]. In this study, the criterion values were set to the mean O_3 (representative pollutant) concentrations of each stage and the PSCF was weighted by the empirical weight value determined by the number of endpoints of air mass trajectories in the grid (W_{ij}). The domain was in the range of 30-55°N and 75-120°E with more than 95% of the back trajectories in the geographic areas and the resolution was $0.5^\circ \times 0.5^\circ$.

$$W_{ij} = \begin{cases} 1.00 & n_{ij} > 80 \\ 0.70 & 80 \geq n_{ij} > 20 \\ 0.42 & 20 \geq n_{ij} > 10 \\ 0.05 & n_{ij} < 10 \end{cases}$$

Results and Discussion

Overall Characteristics of General Air Pollutants and Meteorological Factors

Hourly concentrations of PM_{10} , $PM_{2.5}$, SO_2 , NO_2 , CO and O_3 are illustrated in Fig. 2. Daily values of meteorological parameters are shown in Fig. 3. Fig. 4 and Table 2 show the staged variation of the six pollutants based on their daily average concentrations. Daily average concentration of O_3 was set as the highest average of the measured ozone from eight consecutive hours in a day and referred to as O_3 -8 hr [13].

From Fig. 2, the variation tendencies of PM_{10} , $PM_{2.5}$, SO_2 , NO_2 and CO were consistent with each other, while O_3 showed the reverse change trend.

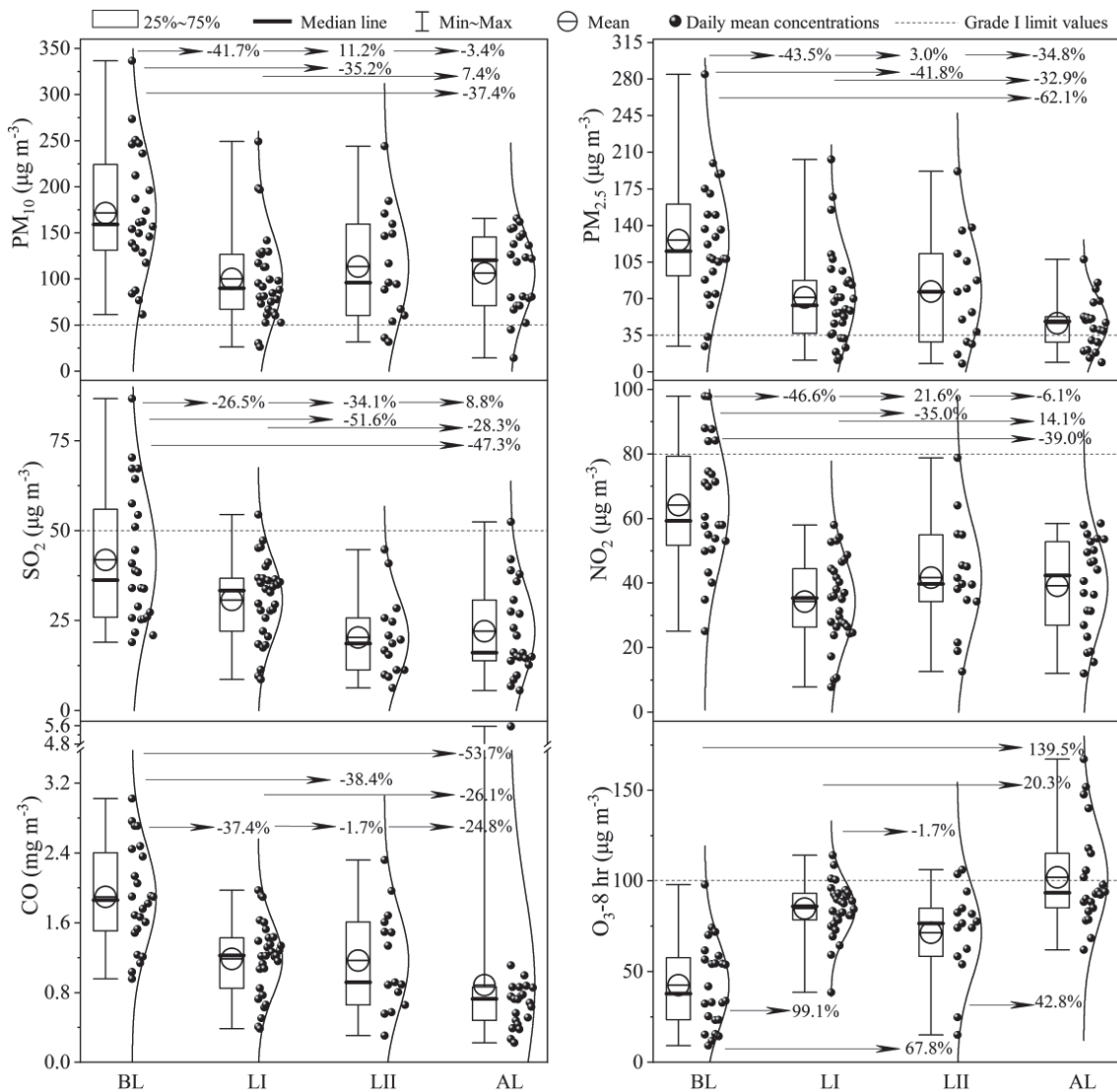


Fig. 4. Daily average concentrations (circles) with median values (thicker lines), the distances between the first and third quartiles (boxplots) and the minimum and maximum values (whiskers) of PM_{10} , $PM_{2.5}$, SO_2 , NO_2 , CO and O_3 before lockdown (BL), during lockdown in the 1st stage (LI) and the 2nd stage (LII), and after lockdown (AL), respectively. The percentages followed the arrows indicate the variations between the stages. The curves represent the normal distributions of the data (ball). The numbers of the data in BL, LI, LII and AL were 24, 30, 15 and 22, respectively.

Table 2. Daily average mass concentrations ($\mu\text{g m}^{-3}$) of each air pollutants in different areas.

Pollutants	BL	LI	LII	AL	All stages	Grade I values
PM ₁₀	171.58	100.06	111.24	107.46	122.60	50
PM _{2.5}	126.08	71.22	73.33	47.78	80.65	35
SO ₂	41.84	30.74	73.33	22.05	29.84	50
NO ₂	64.17	34.29	41.68	39.12	44.55	80
CO	1900	1190	1170	880	1300	4000
O ₃ -8hr	42.55	84.73	71.39	101.92	75.56	100

PM₁₀, PM_{2.5}, SO₂, NO₂ and CO underwent remarkable reductions during and after the lockdown while O₃ pollution was generally amplified during the lockdown in Taiyuan. During the period of observation, the average daily mass concentrations of PM₁₀, PM_{2.5}, SO₂, NO₂, CO and O₃-8hr in Taiyuan were 122.60, 80.65, 29.84, 44.55, 1.30×10³ and 75.56 $\mu\text{g m}^{-3}$, respectively (Table 2). Although the decrease of the five pollutants were underwent in Taiyuan from an overall lockdown stages, it was quite apparent that the mass concentrations of both PM₁₀ and PM_{2.5} greatly exceeded the daily average Grade I limit (DAILVs, 50 $\mu\text{g m}^{-3}$ and 35 $\mu\text{g m}^{-3}$) of the Ambient Air Quality Standard of China (CAAQS, GB 3095-2012) in all stages (Fig. 2, 4 and Table 2) and the days of PM₁₀ and PM_{2.5} concentrations exceeded the daily average Grade I limit were 85 and 72, respectively (Fig. 4), which indicated that Taiyuan was suffering from heavy particulate matters pollution during the study period and were also reflected in visibility (Fig. 3). In addition, the average mass concentrations O₃-8 hr during the AL stage (101.92 $\mu\text{g m}^{-3}$) exceeded the Grade I limiting value (100 $\mu\text{g m}^{-3}$). It can be seen that the weather conditions in Taiyuan were basically stable, the wind speed is low (<2 m/s), the relative humidity is moderate (51.2%), and the average solar irradiance and daily hours of sunlight gradually increased during the observation period (Table 1 and Fig. 3).

Staged Characteristics of Pollutants

PM₁₀, PM_{2.5}, SO₂, NO₂ and CO

From Fig. 4 and Table 2, PM₁₀, PM_{2.5}, SO₂, NO₂ and CO experienced a more significant reduction from the period of BL to LI and mixed variations from LI to LII and AL. The average concentrations decreased from 171.58, 126.08, 41.84, 64.17 and 1.9×10³ $\mu\text{g m}^{-3}$ in BL stage to 100.06, 71.22, 30.74, 34.29 and 1.19×10³ $\mu\text{g m}^{-3}$ in LI stage for PM₁₀, PM_{2.5}, SO₂, NO₂ and CO, respectively, with different rate fall, which saw 41.7%, 43.5%, 26.5%, 46.6% and 37.4% drops. Of them, the NO₂ emissions reduced the highest, which are comparable to the reductions observed in Milan (45.6%) in Italy [22], Almaty (49%) in Kazakhstan [23] and Kolkata (47%) in India [24] and lower than those in Wuhan (53.3%) [25] and Shanghai (59.1%) [26] in

China, Delhi (60.1%) and Mumbai (78.1%) in India [24] (Table 3). From the period of LI to LII, marked and slight reductions occurred for SO₂ (34.1%) and CO (1.7%) while PM₁₀ (11.2%), PM_{2.5} (3.0%) and NO₂ (21.6%) had varying degrees of increase. Except SO₂ with a slight increase of 8.8%, the AL stage marked further decreases in PM₁₀ (3.4%), PM_{2.5} (34.8%), NO₂ (6.1%) and CO (24.8%) compared to the LII. Additionally, we found that the proportions of changes in different air pollutants vary greatly. In different stages, that largely was due to the pollution source of different pollutants. It is known that coarse particles (PM₁₀) in the megacities are mainly composed of man-made fugitive dust from natural dust from the ground, industrial activities and roads, growth of secondary aerosol particles, and construction activities in urban areas [27] and biomass burning, industrial emissions fossil fuel combustion, and vehicle emissions are the main anthropogenic sources of PM_{2.5} [6, 10, 22, 28]. The main sources of CO emissions are incomplete combustion processes, such as transportation, home heating [22]. Great decrease and slightly increase in SO₂ during the lockdown (LI and LII) and AL stages suggested SO₂ control was effective during lockdown and normal days. Industrial and coal-fired power plants were the primary sources of SO₂ in Taiyuan city. NO₂ entered the atmosphere mainly from both the burning of fossil fuels and the photochemical oxidation of nitric oxide emitted from combustion processes, soils, plants, and so on [6]. Since pollutants SO₂, NO₂ and CO are emitted directly from the local sources, their concentrations were more affected by the regional sources relative to O₃ and PM_{2.5} [29]. Therefore, the pollution mitigation in Taiyuan during LI was mainly due to restrictions on industrial activities and transportation. The inconsistent patterns of these five air pollutants during LII and AL stages suggested the important contributions of factitious factors and impacts of regional transport during the lockdown. We observed that the slight increase and then great decrease in NO₂ and PM_{2.5} concentrations occurred during LII stage and AL stages due to the production intensity is higher than the BL period, which made up the production deficiency during the COVID-Lockdown period. Additionally, the slight changes above might be ascribed to the numbers and dispersion of data as shown in Fig. 4.

O₃

The level of urban air pollution is mainly affected by local emissions and chymic mechanisms [30]. Pollution mitigations were expected, because it is consistent with typical fluctuations in energy demand before, during, and after lockdown. However, on the contrary to other pollutants above, unexpected O₃ pollution was generally amplified during lockdown in Taiyuan. As shown in Fig. 4, compared to BL stage, O₃ exhibited a more marked increase in LI (99.1%), LII (67.8%) and AL (139.5%) stages, which was consistent with the recent literature. Table 3 summarized the percent drop and rise of the above five air pollutants and O₃ induced by lockdown in Taiyuan and other cities of China and other countries. Take O₃ for example, ambient O₃ levels increased around the lockdown i.e. 116.6%, 145% and 20.5% in Wuhan (the city that COVID-19 initially identified) [11], Hangzhou [10] and the Yangtze River Delta Region (YRDR) [31], China, 20.7%, 35.1%, 37.4% and 66.1% in Mumbai, Singrauli, Delhi [24] and Kolkata [32], India, 40% 50%, 26.9% and 30.4% in California, New York, Ohio and Washington, USA, [33], 15%

in Almaty, Kazakhstan [23], 169.9% in Milan, Italy [22] and 30% in Sao Paolo, Brazil [34]. Widespread O₃ pollution occurred during the lockdown indicated that the generation of O₃ should be influenced not only by emission reduction and also multiple factors else.

Correlations Among Air Pollutants and Meteorological Parameters

The cross relationships (Spearman’s rank) among the six air pollutants (PM₁₀, PM_{2.5}, SO₂, NO₂, CO and O₃) and the five meteorological factors (T, RH, WS, V, SI) based on daily mean data during the sampling period infer the pollutants’ possible common sources and the influence by the meteorological conditions and illustrated in Fig. 5.

Correlations Among Air Pollutants

As Fig. 5 shown, the strong positive correlations among PM₁₀, PM_{2.5}, SO₂, NO₂ and CO were found, implying the common local dominant sources, such as fossil fuels combustion [35, 36]. CO had good positive

Table 3. Comparison of percent (%) changes of each air pollutants induced by lockdown in different areas.

Areas		PM ₁₀	PM _{2.5}	SO ₂	NO ₂	CO	O ₃	References	
Taiyuan	China	-41.7	-43.5	-26.5	-46.6	-37.4	99.1	This work	
Wuhan		-40.2	-36.9	-3.9	-53.3	-(3.2~34.5)	116.6	[25]	
Beijin-Tianjin-Hebei		-13.7	-5.9	-6.8	-24.7	-4.6		[52]	
Shanghai			-40.9	-24.6	-59.1		24.2	[26]	
Hefei				-44.8	-27.1	-65.2	17.5		
Nanjing				-35.9	-27.5	-42.7	4.6		
Suzhou				-37.4	-27.3	-56.4	12.3		
Hangzhou				-38.5	-32.9	-50.5	8.2		
Shaoxing				-40.4	-32.0	-42.8	0		
Hangzhou			-54	-59	-22	-82*	-27	125	[28]
Delhi		India	-55.0	-49.3	-19.5	-60.1		37.4	[24]
Mumbai	-44.6		-37.4	-39.0	-78.1		20.7		
Singrauli	58.9		15.3	11.8	-12.5		35.1		
Kolkata	-44.9		-41.2	42.3	-47.7	-16.4	66.1	[32]	
Delhi	-52		-41		-50	-29	7	[53]	
Mumbai	-47		-33		-75	-46	8		
Kolkata	-34		-23		-60	-29	17		
California	USA	-63.9	-63.3		-66.7	-55.6	40	[33]	
New York			-45.3		-55.1	-48.3	50		
Ohio		19.0	4.7		-30.6	-4.8	26.9		
Washington			14.7		-28.6	-13.6	30.4		
Milan	Italy	-39.5	-37.1	-19.9	-43.1	-45.6	169.9	[22]	
Almaty	Kazakhstan		-21	7	-35	-49	15	[23]	
Sao Paolo	Brazil		-29.8		-54.3	-64.8	30	[54]	

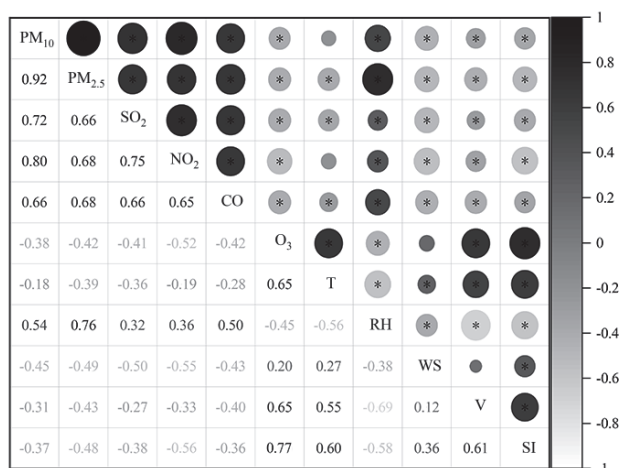


Fig. 5. Spearman's rank correlations among air pollutants and meteorological parameters (* $p < 0.05$).

correlations with PM₁₀ (0.66), PM_{2.5} (0.68), SO₂ (0.66) and NO₂ (0.65) and negative correlation with O₃ (-0.42), suggesting the primary emissions from industrial and traffic emissions were relatively dominated the local pollution. O₃ had strong adverse correlations with the other five pollutants and had the most robust relationship with NO₂ (-0.52) and comparative relationships with the other four pollutants, suggesting precursor consumption and oxide formation. According to the recent studies, the unprecedented reduction in NO₂ [30, 37, 38] and PM_{2.5} [28, 37] emissions were considered as main or partial causes of increase in O₃ concentrations during the lockdown, which was in consistent with that in this work. The levels of ambient O₃ and NO₂ were inextricably linked with non-linear relationship (Fig. 6) because of the chemical coupling of O₃ and NO_x (NO + NO₂) and the increment in the level of O₃ was accompanied by a resultant reduction in the level of NO₂ [38-40]. O₃ had stronger negative correlations with the PM_{2.5} (-0.42) than PM₁₀ (-0.38), mainly because the growth of secondary aerosol particles contributed to PM_{2.5} more than PM₁₀ in the megacities and the reduction of PM_{2.5} was conducive to the formation of O₃ [6, 22, 27, 41] which promoted the increase in O₃ during the lockdown period [28]. Additionally, the reduced NO₂ lead to enhancement of O₃ in urban areas of Taiyuan, further increasing the atmospheric oxidizing capacity and promoting the formation of secondary aerosol because of nonlinear production chemistry and titration of ozone in winter [37].

Correlations between Air Pollutants and Meteorological Factors

Meteorological factors have a crucial influence on the accumulation, diffusion and removal of atmospheric pollutants [36]. As shown in Fig. 5, the concentrations of PM_{2.5}, SO₂, NO₂ and CO had a negative correlation with temperature. High temperature may decrease

temperature stratification stability, promote vertical movement of air pollutants [42], and cause dilution and diffusion of air pollutants [43]. O₃ were positively correlated with temperature, with a correlation coefficient of 0.65. This was due to the high temperature leading to the occurrence of photochemical reactions, causing the accumulation of ground-level O₃ [44]. PM₁₀, PM_{2.5}, SO₂, NO₂ and CO were positively correlated with relative humidity, and the correlation coefficients were 0.76, 0.54, 0.32, 0.36 and 0.50, respectively. High relative humidity can increase the concentration of PM by promoting the distribution of semi-volatile substances into the aerosol phase. A humid atmosphere is usually accompanied by a lower boundary layer, which further increases the concentration of pollutants from the main source [45]. At the same time, all air pollutants except O₃ were negatively correlated with wind speed and visibility. Breeze were the cause of weak dilution of primary pollutants, which accelerates the formation and accumulation of secondary PM [35, 46]. On the contrary, strong winds increase the dispersion and dilution of pollutants, flushing PM pollutants out of the city [47]. From Fig. 5, with the exception of PM_{2.5}, PM₁₀, SO₂, NO₂ and CO, O₃ had very weak positive correlation with wind speed with the correlation coefficient of 0.20, which should be ascribed to the different influences between primary and secondary pollutants by weak wind speed during the study period. Besides, the average data of wind speed might not representative of the actual situation and thus the backward trajectories of air masses were discussed below. Subsequently, increased visibility and solar radiation increase O₃ formed by photochemical reactions [48], interpreting that O₃-8hr had positive correlation with visibility (0.65) and solar irradiance (0.77) (Fig. 5). In spring and summer, due to the high solar radiation intensity and daily duration, the photolysis of NO₂ is promoted, and the growth of O₃ is more common [22]. From Fig. 5, besides O₃, the solar irradiance had relatively good negative correlation with NO₂ (-0.56), implying the promotion of photolysis of NO₂. It can also be seen from Fig. 7 which shows

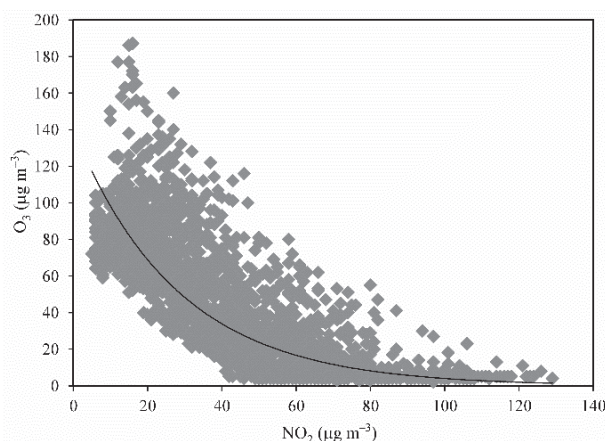


Fig. 6. Scatter diagram of O₃ v.s. NO₂.

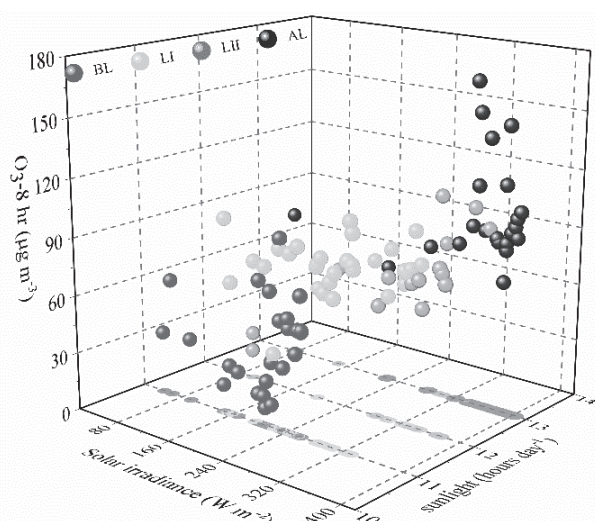


Fig. 7. Daily average concentrations of O₃-8hr as function of daily hours of sunlight and average solar irradiance during daylight hours during BL, LI, LII and AL stages.

the dependence of O₃-8hr concentration in BL, LI, LII and AL on daylight hours and solar radiation, the increases in daylight hours (Table 1) and average solar irradiance during daylight hours might appear crucial factors causing higher O₃ concentrations.

Influence of Air Mass Transport on the Pollutants

Since the significant reduction in the emissions of air pollutants because of the COVID-19 lockdown, air mass transports might play an important role in the concentration of pollutants in the study region. Thus the backward trajectories of air masses at altitudes

of 500 m during the four stages were applied to roughly evaluate the impact of transports on the concentration of air pollutants and illustrated in Fig. 8. As shown, the backward trajectories were divided into four, four, three and three clusters during BL, LI, LII and AL stages, respectively. In the surveyed region, the trajectory clusters during BL stage were made from north (44.79%) with very slow transmission speed of air parcels, indicating the dominated pollutants were mainly from the north of the city, where the Second Power Station and Taiyuan Iron and Steel Factory are located [16]. Another contribution came from southwest (18.75%), where some of the China's top pollution areas (such as Lvliang, Linfen and Yuncheng) are located. A similar situation was in LI stage with 59.81% trajectory clusters from south-southwest. During LII and AL stages, the dominated trajectory clusters were from southeast (46.67% and 32.95%). The south-eastern wind originated from Shandong, Hebei and Henan provinces and passed through Fenhe Plain, transporting pollutants from high-concentration areas [27, 49, 50] in to Taiyuan. To a certain extent, due to the bowl-shaped geographical topography [4], air parcels from west-south-east regions swept across the Fenhe Plain and carried the pollutants to Taiyuan, where the surrounding mountains slowed down the speed of transmission, leading to increased pollutants. The trajectory clusters from northwest gradually increased during LI (40.19%), LII (53.33%) and AL (61.04%) compared to BL (36.46%) may dilute local atmospheric pollutants, which should be part of the reason for the decrease in the concentration of the five pollutants. However, the gradual increase of O₃ levels during the four stages suggested considerable partial precursors of O₃ were from outside of the study area.

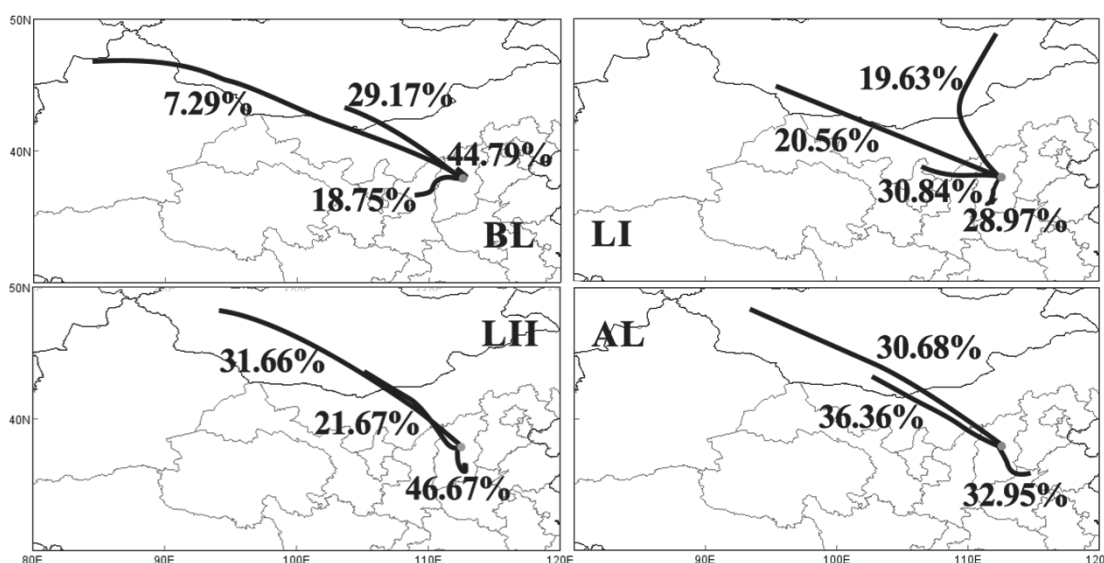


Fig. 8. Staged clusters of 48 h backward trajectories starting at Taiyuan (receptor site is marked by dot) at 500 m altitudes and the percentage of allocation to each cluster.

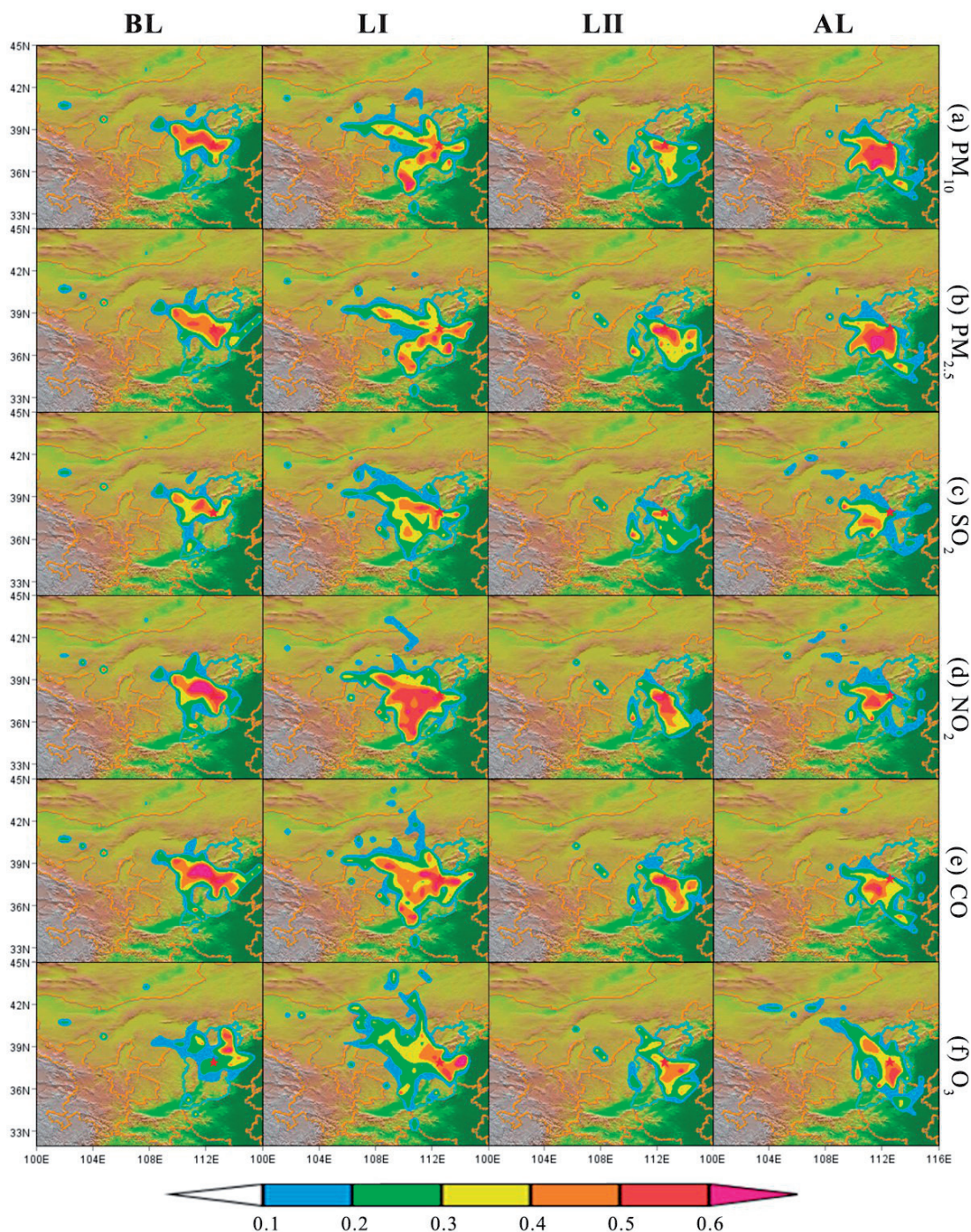


Fig. 9. Staged weighted PSCF distributions of O_3 in Taiyuan (the receptor site is marked by red star).

Furthermore, the horizontal distributions of the weighted PSCF values for the six pollutants were calculated by combining the backward trajectories with their hourly values and are presented in Fig. 9. As depicted, the local emissions were significant for those primary pollutants such as PM_{10} , $PM_{2.5}$, SO_2 , NO_2 and CO and the same patterns were found among them. The potential sources for them showed distinct staged variations such as the northwestern area of Shanxi Province and the northeastern regions of Shaanxi Province during BL stage, and the southwest-southeastern regions during lockdown other stages

(Fig. 9a-e). In terms of O_3 (Fig. 9f), the local photochemistry was enhanced during lockdown period because strong photochemical reactivity. The potential source of O_3 should be explained carefully since it is not directly emitted into the atmosphere and has complex chemical properties with VOCs and NO_x [51]. The majority of the O_3 might be formed by photooxidation near the receptor site. Local emission of precursors of O_3 was very low during BF stage and gradually increased during LI, LII and AL stages. In addition, high O_3 concentration during BL stage were connected with air masses coming from northeastern

regions such as the northern part of Shanxi Province and the eastern part of Hebei Province while higher O₃ concentrations during LI, LII and AL stages were connected with air masses coming from southeastern regions such as Hebei, Henan and Shandong Province, which was in line with discussions on the trajectory clusters.

Conclusions

In this study, PM₁₀, PM_{2.5}, SO₂, NO₂, CO, O₃ as well as meteorological parameters have been investigated before, during and after the COVID-19 lockdown in the early 2020 and the main conclusions are summarized.

The average mass concentrations of PM₁₀, PM_{2.5}, NO₂, SO₂, CO and O₃ in Taiyuan were 122.60, 80.65, 29.84, 44.55, 1.30×10³ and 75.56 μg m⁻³, respectively. The average mass concentrations of PM₁₀ and PM_{2.5} in all stages were greatly exceeded the daily average level I limit of CAAQS. The average mass concentrations O₃-8hr during the AL stage (101.92 μg m⁻³) exceeded its Grade I limiting value.

1. PM₁₀ (-41.7%), PM_{2.5} (-43.5%), SO₂ (-26.5%), NO₂ (-46.6%) and CO (-37.4%) underwent a more marked reduction while O₃ (99.1%) pollution was amplified during lockdown.
2. O₃ were negatively correlated with the other pollutants and positively correlated with temperature, visibility and the average solar irradiance during daylight hours. The increases in daylight hours and average solar irradiance during daylight hours might appear crucial factors causing higher O₃ concentrations.
3. The reduction of PM_{2.5} and NO₂ promoted the increase in O₃ during the lockdown period.
4. Most of the O₃ might be formed by photooxidation near Taiyuan and connected with air masses from the northern part of Shanxi Province during BL stage and Henan, Hebei and Shandong Province during LI, LII and AL stages.

Acknowledgments

This work was supported by Fundamental Research Program of Shanxi Province, China (20210302123043, 201601D021135), Postgraduate Education Innovation Project of Shanxi Province, China (2020SY400), Key Research and Development (R&D) Projects of Shanxi Province, China (201803D121035) and National Natural Science Foundation of China (21707125).

Conflict of Interest

The authors declare no competing interests.

References

1. HE H., WANG Y., MA Q., MA J., CHU B., JI D., TANG G., LIU C., ZHANG H., HAO J. Mineral dust and NO_x promote the conversion of SO₂ to sulfate in heavy pollution days. *Scientific Reports* **4**, 4172, **2014**.
2. HUANG J., PAN X., GUO X., LI G. Health impact of China's Air Pollution Prevention and Control Action Plan: an analysis of national air quality monitoring and mortality data. *The Lancet Planetary Health* **2**, e313, **2018**.
3. LIU P., ZHANG C., XUE C., MU Y., LIU J., ZHANG Y., TIAN D., YE C., ZHANG H., GUAN J. The contribution of residential coal combustion to atmospheric PM_{2.5} in northern China during winter. *Atmospheric Chemistry and Physics* **17**, 11503, **2017**.
4. LIU K., REN J. Seasonal characteristics of PM_{2.5} and its chemical species in the northern rural China. *Atmospheric Pollution Research* **11**, 1891, **2020**.
5. GUAN Y., XIAO Y., WANG Y., ZHANG N., CHU C. Assessing the health impacts attributable to PM_{2.5} and ozone pollution in 338 Chinese cities from 2015 to 2020. *Environmental Pollution* **287**, 117623, **2021**.
6. GHAREMANLOO M., LOPS Y., CHOI Y., MOUSAVINEZHAD S. Impact of the COVID-19 outbreak on air pollution levels in East Asia. *Science of the Total Environment* **754**, 142226, **2021**.
7. WHO Coronavirus disease (COVID-19). www.who.int/emergencies/diseases/novel-coronavirus-2019 (available in June 8 2021), **2021**.
8. CHOWDHURY R.B., KHAN A., MAHIAT T., DUTTA H., TASMEEA T., BINTH ARMAN A.B., FARFU F., ROY B.B., HOSSAIN M.M., KHAN N.A., AMIN A., SUJAUDDIN M. Environmental externalities of the COVID-19 lockdown: Insights for sustainability planning in the Anthropocene. *Science of the Total Environment* **783**, 147015, **2021**.
9. ZHENG H., KONG S., CHEN N., YAN Y., LIU D., ZHU B., XU K., CAO W., DING Q., LAN B., ZHANG Z., ZHENG M., FAN Z., CHENG Y., ZHENG S., YAO L., BAI Y., ZHAO T., QI S. Significant changes in the chemical compositions and sources of PM_{2.5} in Wuhan since the city lockdown as COVID-19. *Science of the Total Environment* **739**, 140000, **2020**.
10. WANG L., LI M., YU S., CHEN X., LI Z., ZHANG Y., JIANG L., XIA Y., LI J., LIU W., LI P., LICHTFOUSE E., ROSENFELD D., SEINFELD J.H. Unexpected rise of ozone in urban and rural areas, and sulfur dioxide in rural areas during the coronavirus city lockdown in Hangzhou, China: implications for air quality. *Environmental Chemistry Letters* **18**, 1713, **2020**.
11. LIAN X., HUANG J., HUANG R., LIU C., WANG L., ZHANG T. Impact of city lockdown on the air quality of COVID-19-hit of Wuhan city. *Science of the Total Environment* **742**, 140556, **2020**.
12. WANG M., CHEN W., ZHANG L., QIN W., ZHANG Y., ZHANG X., XIE X. Ozone pollution characteristics and sensitivity analysis using an observation-based model in Nanjing, Yangtze River Delta Region of China. *J Environ Sci (China)* **93**, 132, **2020**.
13. FENG R., LUO K., FAN J.-R. Decoding Tropospheric Ozone in Hangzhou, China: from Precursors to Sources. *Asia-Pacific Journal of Atmospheric Sciences* **56**, 321, **2019**.
14. IPCC (Intergovernmental Panel on Climate Change). AR5 Climate Change 2013. Available: <https://www.ipcc.ch/report/ar5/wg1/> Accessed, November 11, **2020**.

15. JAKOVLJEVIC T., LOVRESKOV L., JELIC G., ANAV A., POPA I., FORNASIER M.F., PROIETTI C., LIMIC I., BUTORAC L., VITALE M., DE MARCO A. Impact of ground-level ozone on Mediterranean forest ecosystems health. *Science of the Total Environment* **783**, 147063, **2021**.
16. LIU K., SHANG Q., WAN C., SONG P., MA C., CAO L. Characteristics and Sources of Heavy Metals in PM_{2.5} during a Typical Haze Episode in Rural and Urban Areas in Taiyuan, China. *Atmosphere* **9**, 2, **2018**.
17. ZHANG Z., ZHANG Y., WANG X., Lü S., HUANG Z., HUANG X., YANG W., WANG Y., ZHANG Q. Spatiotemporal patterns and source implications of aromatic hydrocarbons at six rural sites across China's developed coastal regions. *Journal of Geophysical Research: Atmospheres* **121**, 6669, **2016**.
18. WANG Y. *MeteoInfo: meteorological GIS, scientific computation and visual platform*. Beijing: China Meteorological Press, **2021**.
19. CHAO S., LIU J., CHEN Y., CAO H., ZHANG A. Implications of seasonal control of PM_{2.5}-bound PAHs: An integrated approach for source apportionment, source region identification and health risk assessment. *Environmental Pollution* **247**, 685, **2019**.
20. REN B., XIE P., XU J., LI A., TIAN X., HU Z., HUANG Y., LI X., ZHANG Q., REN H., JI H. Use of the PSCF method to analyze the variations of potential sources and transports of NO₂, SO₂, and HCHO observed by MAX-DOAS in Nanjing, China during 2019. *Science of The Total Environment* **782**, 146865, **2021**.
21. WANG Y.Q. The transport pathways and sources of PM10 pollution in Beijing during spring 2001, 2002 and 2003. *Geophysical Research Letters* **31**, L14110, **2004**.
22. COLLIVIGNARELLI M.C., ABBÀ A., BERTANZA G., PEDRAZZANI R., MIINO M.C. Lockdown for COVID-2019 in Milan: What are the effects on air quality? *Science of The Total Environment* **732**, 139280, **2020**.
23. KERIMRAY A., BAIMATOVA N., IBRAGIMOVA O.P., BUKENOV B., KENESSOV B., PLOTITSYN P., KARACA F. Assessing air quality changes in large cities during COVID-19 lockdowns: The impacts of traffic-free urban conditions in Almaty, Kazakhstan. *Science of the Total Environment* **730**, 139179, **2020**.
24. KUMARI P., TOSHNIWAL D. Impact of lockdown measures during COVID-19 on air quality – A case study of India. *International Journal of Environmental Health Research* 1-8, **2020**.
25. LIAN X., HUANG J., UANG R.H., LIU C., ZHANG T. Impact of city lockdown on the air quality of COVID-19-hit of Wuhan city. *Science of The Total Environment* **742**, 140556, **2020**.
26. LI L., LI Q., HUANG L., WANG Q., CHAN A. Air quality changes during the COVID-19 lockdown over the Yangtze River Delta Region: An insight into the impact of human activity pattern changes on air pollution variation. *Science of The Total Environment* **732**, 139282, **2020**.
27. GUO X., WU H., CHEN D., YE Z., SHEN Y., LIU J., CHENG S. Estimation and prediction of pollutant emissions from agricultural and construction diesel machinery in the Beijing-Tianjin-Hebei (BTH) region, China. *Environmental Pollution* **260**, 113973, **2020**.
28. YUAN Q., QI B., HU D., WANG J., ZHANG J., YANG H., ZHANG S., LIU L., XU L., LI W. Spatiotemporal variations and reduction of air pollutants during the COVID-19 pandemic in a megacity of Yangtze River Delta in China. *Science of the Total Environment* **751**, 141820, **2021**.
29. YU S., ZHANG Q., YAN R., WANG S., LI P., CHEN B., LIU W., ZHANG X. Origin of air pollution during a weekly heavy haze episode in Hangzhou, China. *Environmental Chemistry Letters* **12**, 543-550, **2014**.
30. SICARD P., DE MARCO A., AGATHOKLEOUS E., FENG Z., XU X., PAOLETTI E., RODRIGUEZ J.J.D., CALATAYUD V. Amplified ozone pollution in cities during the COVID-19 lockdown. *Science of the Total Environment* **735**, 139542, **2020**.
31. LI L., LI Q., HUANG L., WANG Q., ZHU A., XU J., LIU Z., LI H., SHI L., LI R., AZARI M., WANG Y., ZHANG X., LIU Z., ZHU Y., ZHANG K., XUE S., OOI M.C.G., ZHANG D., CHAN A. Air quality changes during the COVID-19 lockdown over the Yangtze River Delta Region: An insight into the impact of human activity pattern changes on air pollution variation. *Science of the Total Environment* **732**, 139282, **2020**.
32. SATHE Y., GUPTA P., BAWASE M., LAMSAL L., PATADIA F., THIPSE S. Surface and satellite observations of air pollution in India during COVID-19 lockdown: Implication to air quality. *Sustainable Cities and Society* **66**, 102688, **2021**.
33. CHEN L., CHIEN L.C., LI Y., LIN G. Nonuniform impacts of COVID-19 lockdown on air quality over the United States. *Science of The Total Environment* **745**, 141105, **2020**.
34. NAKADA L.Y.K., URBAN R.C. COVID-19 pandemic: Impacts on the air quality during the partial lockdown in Sao Paulo state, Brazil. *Science of the Total Environment* **730**, 139087, **2020**.
35. WANG Y., YING Q., HU J., ZHANG H. Spatial and temporal variations of six criteria air pollutants in 31 provincial capital cities in China during 2013-2014. *Environment International* **73**, 413, **2014**.
36. LIU L., MA X., WEN W., SUN C., JIAO J. Characteristics and potential sources of wintertime air pollution in Linfen, China. *Environmental Monitoring and Assessment* **193**, 252, **2021**.
37. LE T., WANG Y., LIU L., YANG J., YUNG Y.L., LI G., SEINFELD J.H. Unexpected air pollution with marked emission reductions during the COVID-19 outbreak in China. *Science* **369**, 702, **2020**.
38. CLAPP L.J., JENKIN M.E. Analysis of the relationship between ambient levels of O₃, NO₂ and NO as a function of NO_x in the UK. *Atmospheric Environment* **35**, 6391, **2001**.
39. HAMODA M.F., AL-JARALLA R., AL-MAHAMEL S. Assessment of air pollutants emissions due to traffic in two residential areas in Kuwait. *International Journal of Environmental Science and Technology* **2020**.
40. MERTENS M., JÖCKEL P., MATTHES S., NÜTZEL M., GREWE V., SAUSEN R. COVID-19 induced lower-tropospheric ozone changes. *Environmental Research Letters* **16**, **2021**.
41. LI K., JACOB D.J., LIAO H., SHEN L., ZHANG Q., BATES K.H. Anthropogenic drivers of 2013-2017 trends in summer surface ozone in China. *Proceedings of the National Academy of Sciences of the United States of America* **116**, 422, **2019**.
42. MOR S., KUMAR S., SINGH T., DOGRA S., PANDEY V., RAVINDRA K. Impact of COVID-19 lockdown on air quality in Chandigarh, India: Understanding the emission sources during controlled anthropogenic activities. *Chemosphere* **263**, 127978, **2021**.

43. LI X.L., MA Y.J., WANG Y.F., LIU N.W., HONG Y. Temporal and spatial analyses of particulate matter (PM₁₀ and PM_{2.5}) and its relationship with meteorological parameters over an urban city in northeast China. *Atmospheric Research* **198**, 185, **2017**.
44. COATES J., MAR K.A., OJHA N., BUTLER T.M. The influence of temperature on ozone production under varying NO_x conditions - a modelling study. *Atmospheric Chemistry and Physics* **16**, 11601, **2016**.
45. HOSHINO T., HOSHINO A., NISHINO J. Relationship between environment factors and the number of outpatient visits at a clinic for nonallergic rhinitis in Japan, extracted from electronic medical records. *European Journal of Medical Research* **20**, 17, **2015**.
46. WANG M., CAO C., LI G., SINGH R.P. Analysis of a severe prolonged regional haze episode in the Yangtze River Delta, China. *Atmospheric Environment* **102**, 112, **2015**.
47. LIU L., MA X., WEN W., SUN C., JIAO J. Characteristics and potential sources of wintertime air pollution in Linfen, China. *Environmental Monitoring and Assessment* **193**, 252, **2021**.
48. RUI L., CUI L., LI J., AN Z., CHEN J. Spatial and temporal variation of particulate matter and gaseous pollutants in China during 2014-2016. *Atmospheric Environment* **161**, 235, **2017**.
49. SUN M., ZHOU Y., WANG Y., ZHENG X., CUI J., ZHANG D., ZHANG J., ZHANG R. Seasonal discrepancies in peroxyacetyl nitrate (PAN) and its correlation with ozone and PM_{2.5}: Effects of regional transport from circumjacent industrial cities. *Science of the Total Environment* **785**, 147303, **2021**.
50. LV D., LU S., TAN X., SHAO M., XIE S., WANG L. Source profiles, emission factors and associated contributions to secondary pollution of volatile organic compounds (VOCs) emitted from a local petroleum refinery in Shandong. *Environ Pollut* **274**, 116589, **2021**.
51. ZHANG G., XU H., QI B., DU R., GUI K., WANG H., JIANG W., LIANG L., XU W. Characterization of atmospheric trace gases and particulate matter in Hangzhou, China. *Atmospheric Chemistry and Physics* **18**, 1705, **2018**.
52. BAO R., ZHANG A. Does lockdown reduce air pollution? Evidence from 44 cities in northern China. *Science of The Total Environment* **731**, 139052, **2020**.
53. JAIN D.S., SHARMA T. Social and Travel Lockdown Impact Considering Coronavirus Disease (COVID-19) on Air Quality in Megacities of India: Present Benefits, Future Challenges and Way Forward. *Aerosol and Air Quality Research* **2020**.
54. NAKADA L., URBAN R.C. COVID-19 pandemic: Impacts on the air quality during the partial lockdown in So Paulo state, Brazil. *Science of The Total Environment* **730**, 139087, **2020**.